Compact stars with dense quark cores: EoS, composition and evolution

Armen Sedrakian

ITP, Goethe-Universität, Frankfurt am Main

Hirschegg, 19 January, 2016

Structure of this talk

1. Introduction to structure of compact stars with dense quark cores (Bonanno and AS, 2012 + extension to $T \neq 0$, 2016)
2. Transport formalism and complete coefficients for the 2SC phase (Nishimura, Alford, AS, 2014)
3. Thermal evolution and Cas A as a phase transition in QCD phase diagram (AS 2015)
4. Summary

I. Compact stars with dense quark cores

Neutron stars as probes of dense matter

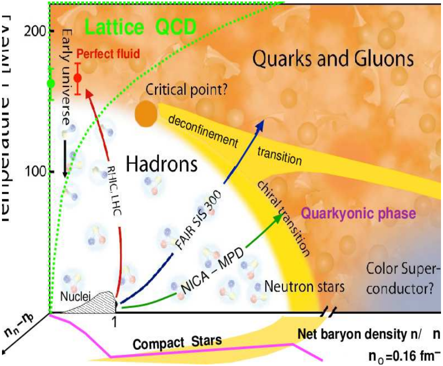

Neutron stars and supernovae provide complementary information on the state of matter at very high densities to that one hopes to gain from future experiments such as FAIR and NICA.

General form of order parameter

$$\Delta \propto \langle 0|\psi^a_{\alpha\sigma}\psi^b_{\beta\tau}|0\rangle$$

- Antisymmetry in spin σ, τ for the BCS mechanism to work
- Antisymmetry in color a, b for attraction
- Antisymmetry in flavor α, β to avoid Pauli blocking

At low densities 2SC phase (Bailin and Love ’84)

$$\boxed{\Delta(2SC) \propto \Delta\epsilon^{ab3}\epsilon_{\alpha\beta}}$$

Important variations on 2SC phase (crystalline-color-superconductor)

$$\boxed{\Delta(CSC) \propto \Delta\epsilon^{ab3}\epsilon_{\alpha\beta}, \qquad \delta\mu \neq 0, \qquad m_s \neq 0.}$$

At high densities we expect 3 flavors of u, d, s massless quarks. The ground state is the color-flavor-locked phase

$$\boxed{\Delta(CFL) \propto \langle 0|\psi^a_{\alpha L}\psi^b_{\beta L}|0\rangle = -\langle 0|\psi^a_{\alpha R}\psi^b_{\beta R}|0\rangle = \Delta\epsilon^{abC}\Delta\epsilon_{\alpha\beta C}}$$

Phase diagram in NJL see Buballa-Shovkovy-Rischke, Sandin-Blaschke, ... (2006+)

EOS with equilibrium between nuclear, hypernuclear, 2SC and CFL phases of matter

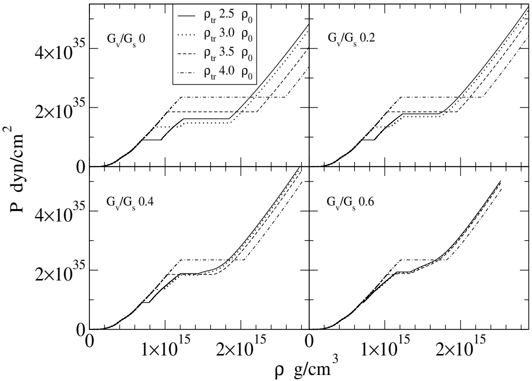

- Phase equilibrium is constructed via Maxwell prescription
- Sequential phase transition $NM \rightarrow 2SC \rightarrow CFL$

see Bonanno and Sedrakian (2012) and 100+ similar calculations 2013-2016

Internal structure of hybrid massive $\sim 1.9M_{\odot}$ star with color superconducting phases

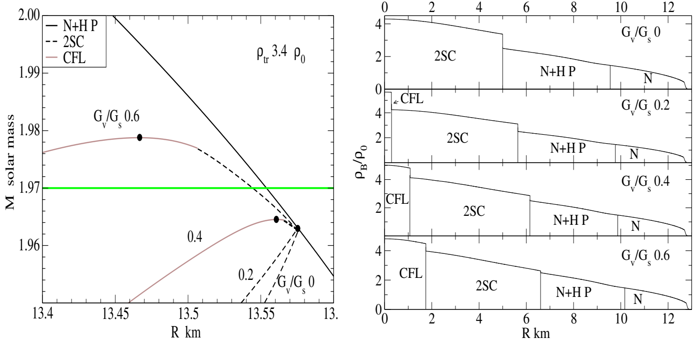

- Small G_V 2SC only. For lagre G_V CFL phase appears.
- Stability is achieved for $G_V > 0.2$ and transition densities few ρ_0

II. Transport coefficients of dense quark matter: Variational calculation

Boltzmann equation for fermions:

$$\left(\frac{\partial}{\partial t} + \mathbf{v}_1 \cdot \nabla_{\mathbf{x}}\right) f_1 = -(2\pi)^4 \sum_j \nu_j \sum_{234} |M_{ij}|^2 \times [f_1 f_2 (1-f_3)(1-f_4) - f_3 f_4 (1-f_1)(1-f_2)]\, \delta^4(p_{\rm in} - p_{\rm out})$$

f - fermion distribution function, M_{ij} scattering matrix element.
ν_j - the degeneracy factors (spin, flavor, color)

What are the degrees of freedom?

Fermions in the basis:

$$\Psi_i = \{\Psi_{bu}, \Psi_{bd}, \Psi_e\} = \{\text{blue up quark } (bu), \text{ blue down quark } (bd), \text{ electron } (e)\}.$$

the indices i and j specify the species of the ungapped fermions in this basis.

Further assumptions:

- Red and green colors are gapped and do not contribute to the transport
- No strangeness (number of s-quarks too small)
- High-density, low-temperature regime $T, m \ll \mu_q$
- Light flavor (isospin) asymmetry typical for neutron stars $\mu_u \ll \mu_d$ (β-equilibrium)

Gauge bosons: write the covariant derivative as

$$\boxed{D_\mu \Psi = \left(\partial_\mu - i \sum_a A^a_\mu Q^a\right)\Psi} \tag{1}$$

Two basis for gauge bosons - standard $(T_8, Q)$and rotated $(X, \tilde{Q})$

$$A_\mu = A^{T_8}_\mu T_8 + A^Q_\mu Q = A^X_\mu X + A^{\tilde{Q}}_\mu \tilde{Q}. \tag{2}$$

related by rotations via mixing angle φ

$$A^X_\mu = \cos\varphi\, A^{T_8}_\mu + \sin\varphi\, A^Q_\mu \tag{3}$$

$$A^{\tilde{Q}}_\mu = -\sin\varphi\, A^{T_8}_\mu + \cos\varphi\, A^Q_\mu \qquad \cos\varphi = \frac{\sqrt{3}g}{\sqrt{e^2 + 3g^2}}. \tag{4}$$

-In the rotated basis the $\tilde{Q}$ charge is massless, i.e., $\tilde{Q}$ color magnetic field penetrates the 2SC phase
-In the rotated basis the X charge is massive, i.e., there is a Meissner effect (more precisely color magnetic flux tubes)

The charges Q^a are defined to be the product of the coupling constant and the charge matrix for the ungapped fermions:

$$\begin{aligned} Q^{T_8} &= g \cdot \mathrm{diag}\left(-\frac{1}{\sqrt{3}}, -\frac{1}{\sqrt{3}}, 0\right) \\ Q^{Q} &= e \cdot \mathrm{diag}\left(+\frac{2}{3}, -\frac{1}{3}, -1\right) \end{aligned} \tag{5}$$

in the standard (T_8, Q) basis and

$$\begin{aligned} Q^{X} &= g\cos\varphi \cdot \mathrm{diag}\left(-\frac{1-2\tan^2\varphi}{\sqrt{3}}, -\frac{1+\tan^2\varphi}{\sqrt{3}}, -\sqrt{3}\tan^2\varphi\right) \\ Q^{\tilde{Q}} &= e\cos\varphi \cdot \mathrm{diag}\,(1, 0, -1) \end{aligned} \tag{6}$$

in the rotated $(X, \tilde{Q})$ basis.

- The longitudinal part of the screening is evaluated in the standard basis
- The transverse part of the screening is evaluated in the rotated basis

Computing the matrix element for scattering: $p_{1i} + p_{2j} \to p_{3i} + p_{4j}$ (flavor i, j)

Standard Feynman rules give:

$$M_{ij} = J^{\mu}_{a,i} \left(D^{ab}_{\mu\nu} \right) J^{\nu}_{b,j} \tag{7}$$

$$J^{\mu}_{a,i} = Q^a_i \bar{u}\left(\mathbf{p}_3\right) \gamma^{\mu} u\left(\mathbf{p}_1\right)/2p_1 \qquad J^{\nu}_{b,j} = Q^b_j \bar{u}\left(\mathbf{p}_4\right) \gamma^{\nu} u\left(\mathbf{p}_2\right)/2p_2 \tag{8}$$

where the most general form of the propagator is given by

$$\left(D^{ab}_{\mu\nu} \right)^{-1} = g_{\mu\nu} \left(\omega^2 - q^2 \right) \delta^{ab} + \Pi^{ab}_{\mu\nu} \tag{9}$$

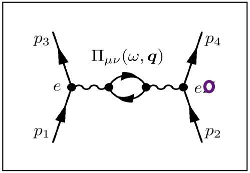

Screening in a plasma is taken into account via self-energies $\Pi_{\mu\nu}$

Decomposition all the quantities (matrix elements, gauge propagators) into longitudinal and transverse parts:

$$M_{ij} = \sum_{a=\{T_8,Q\}} \frac{J^0_{a,i} J^0_{a,j}}{q^2 + \Pi^{aa}_l} - \sum_{a=\{X,\tilde{Q}\}} \frac{\mathbf{J}^t_{a,i} \cdot \mathbf{J}^t_{a,j}}{q^2 - \omega^2 + \Pi^{aa}_t} \tag{10}$$

$$\Pi^{aa}_l = \sum_i \left(q^a_{D,i}\right)^2 \chi_l + 4 \left(q^a_{D,C}\right)^2 \chi_l \qquad \text{in the } (T_8, Q) \text{ basis}$$

$$\Pi^{aa}_t = \sum_i \left(q^a_{D,i}\right)^2 \chi_t + 4 \left(q^a_{D,C}\right)^2 \chi_t + 4 \left(q^a_{D,C}\right)^2 \chi_{sc} \qquad \text{in the } (X, \tilde{Q}) \text{ basis} \tag{11}$$

The screening functions, χ_l and χ_t in the static limit (Hard Thermal Loop approximation)

$$\chi_l = 1, \qquad \chi_t = i\frac{\pi}{4}\frac{\omega}{q}, \qquad \chi_{sc} = \frac{1}{3}. \tag{12}$$

(better done by Rischke and co-workers). To leading order in ω/q, we thus have

$$\Pi_l^{T_8T_8} = \sum_i (Q_i^{T_8})^2 \frac{\mu_i^2}{\pi^2} + 4(Q_C^{T_8})^2 \frac{\mu_C^2}{\pi^2} \tag{13}$$

$$\Pi_l^{QQ} = \sum_i (Q_i^{Q})^2 \frac{\mu_i^2}{\pi^2} + 4(Q_C^{Q})^2 \frac{\mu_C^2}{\pi^2} \tag{14}$$

$$\Pi_t^{XX} = \frac{4}{3}(Q_C^{X})^2 \frac{\mu_C^2}{\pi^2} \tag{15}$$

$$\Pi_t^{\tilde{Q}\tilde{Q}} = i\frac{\omega}{q}\Lambda^2 \qquad \text{where} \quad \Lambda^2 \equiv \sum_i (Q_i^{\tilde{Q}})^2 \frac{\mu_i^2}{4\pi} \tag{16}$$

The Q's can be found in the paper.

The squared matrix element summed over the final spins and averaged over the initial spins is

$$|M_{ij}|^2 = L_l \left| \sum_{a=\{T_8,Q\}} \frac{Q_i^a Q_j^a}{q^2 + \Pi_l^{aa}} \right|^2 + L_t \left| \sum_{a=\{X,\tilde{Q}\}} \frac{Q_i^a Q_j^a}{q^2 - \omega^2 + \Pi_t^{aa}} \right|^2$$
$$-2L_{lt}\, \Re \left[\left(\sum_{a=\{T_8,Q\}} \frac{Q_i^a Q_j^a}{q^2 + \Pi_l^{aa}} \right) \left(\sum_{a=\{X,\tilde{Q}\}} \frac{Q_i^a Q_j^a}{q^2 - \omega^2 + \Pi_t^{aa}} \right)^* \right] + \delta_{ij}\gamma_{\rm int} \qquad (17)$$

where

$$L_l = \left(1 - \frac{q^2}{4p_1^2}\right)\left(1 - \frac{q^2}{4p_2^2}\right)$$
$$L_{lt} = \left(1 - \frac{q^2}{4p_1^2}\right)^{1/2}\left(1 - \frac{q^2}{4p_2^2}\right)^{1/2} \cos\theta \qquad (18)$$
$$L_t = \left(1 - \frac{q^2}{4p_1^2}\right)\left(1 - \frac{q^2}{4p_2^2}\right) \cos^2\theta + \frac{q^2}{4p_1^2} + \frac{q^2}{4p_2^2}$$

The interference γ_{int} term is small and is neglected.

Transport coefficients - definitions of electrical and thermal conductivities and shear viscosity

$$j_\alpha = -\sigma \partial_\alpha U = \int \frac{d^3p}{(2\pi)^3} e v_\alpha \, \delta f \tag{19}$$

$$h_\alpha = -\kappa \partial_\alpha T = \int \frac{d^3p}{(2\pi)^3} (\epsilon - \mu) v_\alpha \, \delta f \tag{20}$$

$$\sigma_{\alpha\beta} = -\eta V_{\alpha\beta} = \int \frac{d^3p}{(2\pi)^3} p_\alpha v_\beta \, \delta f \tag{21}$$

where $V_{\alpha\beta}$ is the traceless part of the spatial derivative of fluid velocity $\mathbf{V}$,

$$V_{\alpha\beta} = \partial_\alpha V_\beta + \partial_\beta V_\alpha - \frac{2}{3}\delta_{\alpha\beta} \nabla \cdot \mathbf{V}. \tag{22}$$

Comparing the left-hand-sides we obtain a universal relation

$$\boxed{\xi Y = \sum_i \nu_i \int \frac{d^3p}{(2\pi)^3} \phi_i \, \delta f_i} \tag{23}$$

where ν_i is a spin factor for a particle flavor i, ξ stands σ, κ, or η, - Y stands $-\partial_\alpha U$, $-\partial_\alpha T$, or $-V_{\alpha\beta}$

Linearization of the Boltzmann equation is given by

$$f_i = f_i^0 + \delta f_i = \frac{1}{e^{(\epsilon-\mu_i)/T}+1} - \frac{\partial f_i^0}{\partial \epsilon}\Phi_i \tag{24}$$

Relaxation time approximation

$$\boxed{\Phi_i = 3\tau_i \psi_i \cdot Y} \tag{25}$$

$$\boxed{\xi_i = -\frac{3\tau_i \nu_i}{\gamma}\int \frac{d^3p}{(2\pi)^3}\,(\phi_i \cdot \psi_i)\,\frac{\partial f_i^0}{\partial \epsilon}} \tag{26}$$

$\gamma = \delta_\alpha^\alpha = 3$ for the electrical and thermal conductivities
$\gamma = \left(\delta_\alpha^\alpha \delta_\beta^\beta + \delta_\alpha^\alpha - 2\delta_\alpha^\alpha/3\right)/2 = 5$ for the shear viscosity. From Eq. (23), we can now define transport coefficient of each component ξ_i as

$$\xi = \sum_i \xi_i = \xi_{bu} + \xi_{bd} + \xi_e \tag{27}$$

Linearization of collision integral

$$\psi_i \cdot Y \frac{\partial f_1^0}{\partial \epsilon_1} = -\frac{(2\pi)^4}{T}\sum_j \nu_j \sum_{234} |M_{ij}|^2 f_1^0 f_2^0 (1-f_3^0)(1-f_4^0)\,\delta^4(p_{\rm in}-p_{\rm out})\,(\Phi_1+\Phi_2-\Phi_3-\Phi_4)\,. \quad (28)$$

Using the same procedure as for the drift term

$$\xi_i = \frac{9\tau_i}{\gamma}\frac{(2\pi)^4}{T}\sum_j \nu_i\nu_j \sum_{1234}|M_{ij}|^2 f_1^0 f_2^0(1-f_3^0)(1-f_4^0)\delta^4(p_{\rm in}-p_{\rm out})\phi_1\cdot[\tau_i(\psi_1-\psi_3)+\tau_j(\psi_2-\psi_4)]\,. \quad (29)$$

In the limit $\omega, T \ll \mu_q$

$$\xi_i = \frac{\tau_i}{\gamma}\sum_j \nu_i\nu_j \frac{36 T\mu_i^2\mu_j^2}{(2\pi)^5}\int_0^\infty d\omega\left(\frac{\omega/2T}{\sinh(\omega/2T)}\right)^2\int_0^{q_M} dq\int_0^{2\pi}\frac{d\theta}{2\pi}|M_{ij}|^2 \phi_1\cdot[\tau_i(\psi_1-\psi_3)+\tau_j(\psi_2-\psi_4)] \quad (30)$$

$q_M = \min[2p_1, 2p_2] = \min[2\mu_i, 2\mu_j]$ is the maximum momentum transfer, and θ is again the angle between $\mathbf{p}_1+\mathbf{p}_3$ and $\mathbf{p}_2+\mathbf{p}_4$. In the limit $T/\mu_q \ll 1$ $p_1, p_2 \to \mu_i, \mu_j$.

Comparing Eqs. (26) and (30) we obtain relaxation times τ_i for the three gapless fermion species.

III. Numerical and analytical results for 2SC phase

Qualitative understanding

- Transport in the 2SC phase occurs via the ungapped fermions: the blue up quark, the blue down quark, and the electron.

- Transport is dominated by the fermion that feels the least influence from surrounding particles (i.e. long relaxation time or mean-free-path)

Relevant interactions

- longitudinal strong interaction (T_8) - Debye screened (short range)
- longitudinal electromagnetic interaction (Q), - Debye screened (short range)
- transverse "rotated" strong interaction (X) - Meissner screening (short ranged)
- transverse "rotated" electromagnetic interaction ($\tilde{Q}$) (not screened, only Landau damped - long ranged at low T)

At low-T the *bu* quark and electron carry $\tilde{Q}$ charge, *bd* does not. Transport is dominated by *bd* quarks (!)

At high T the Landau damping of the $\tilde{Q}$ is more significant. Relaxation times are dominated by the X and T_8 interactions.

Electron, which has no T_8 charge and only a very small X charge, dominates transport.

A transition from the regime dominated by the *bd* quark to a regime dominated by electrons as the temperature is rised.

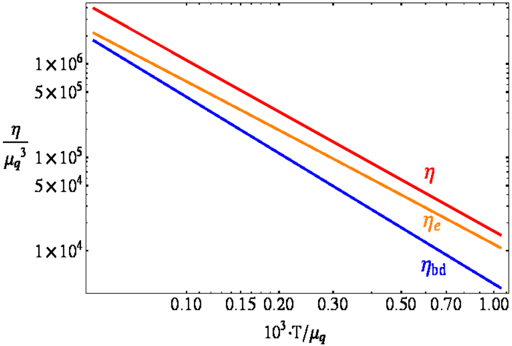

$$\frac{\eta_{bu}}{\mu_q} = \frac{0.150}{(T/\mu_q)^{5/3} + 2490\,(T/\mu_q)^2}, \quad \frac{\eta_e}{\mu_q} = \frac{0.171}{(T/\mu_q)^{5/3} + 2.78\,(T/\mu_q)^2} \tag{31}$$

Numerical calculation of shear viscosity as a function of temperature, taking $\alpha_s = 1$. In this temperature range we see electron and quark contributing equally at high temperature and electron domination at low temperature.

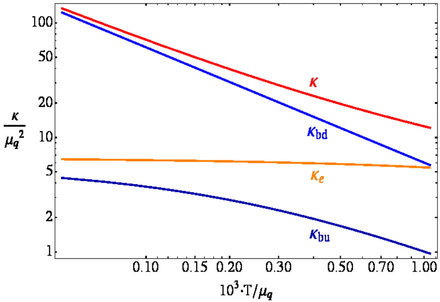

$$\frac{\kappa_{bu}}{\mu_q} = \frac{5.69}{1 + 3720\,(T/\mu_q)}, \quad \frac{\kappa_e}{\mu_q} = \frac{6.70}{1 + 6.92\,(T/\mu_q)^{2/3}} \tag{32}$$

Numerically calculated thermal conductivity in units of quark chemical potential μ_q in the 2SC phase with $\alpha_s = 1$. In this temperature range we see the crossover from electron domination at high temperature to blue down quark domination at low temperature.

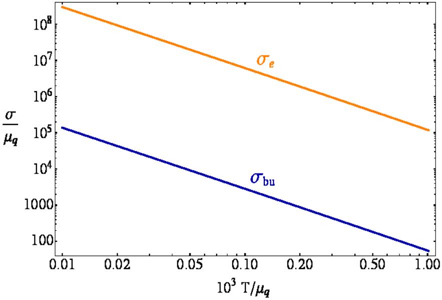

$$\frac{\sigma_{bu}}{\mu_q} = \frac{0.000672}{(T/\mu_q)^{5/3} + 2.11\,(T/\mu_q)^2}, \qquad \frac{\sigma_e}{\mu_q} = \frac{1.46}{(T/\mu_q)^{5/3} + 2.11\,(T/\mu_q)^2} \tag{33}$$

Numerically calculated electrical ($\tilde{Q}$) conductivity as a function of temperature, both expressed in units of the quark chemical potential μ_q, taking strong interaction coupling $\alpha_s = 1$. The electrons dominate because the *bu* relaxation time is shortened by its strong interaction with the *bd* quarks.

Aharonov-Bohm scattering of fermions of color-magnetic flux tubes

AB effect is a quantum-mechanical interference effect: The cross-section (per unit length)

$$\frac{d\sigma}{d\vartheta} = \frac{\sin^2(\pi\beta)}{2\pi k \sin^2(\vartheta/2)}, \quad \beta = \frac{q_p}{q_c}.$$

q_p is the charge of the scattering particle.

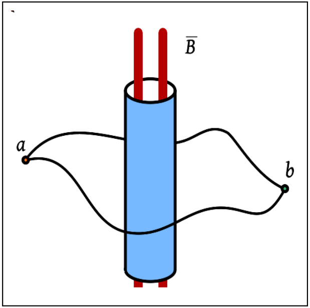

- The cross-section vanishes if β is an integer, but y is otherwise non-zero.
- The cross section is *independent of the thickness of the flux tube*: the scattering is not suppressed in the limit where the symmetry breaking energy scale goes to infinity, and the flux tube thickness goes to zero.

In the complete fermion basis: $\Psi = (ru, gd, rd, gu, bu, bd, e^-)$

$$\beta = \mathrm{diag}\Big(\underbrace{\frac{1}{2}+\frac{e^2}{2g^2}, \frac{1}{2}-\frac{e^2}{2g^2}, \frac{1}{2}-\frac{e^2}{2g^2}, \frac{1}{2}+\frac{e^2}{2g^2},}_{\text{gapped quarks}} -1+\frac{e^2}{g^2}, -1, -\frac{e^2}{g^2}\Big). \quad (34)$$

The bu and electron have a β that differs from an integer by $e^2/g^2 = \alpha/\alpha_s \sim 1/100$, near-maximal Aharonov-Bohm interactions with an X-flux tube, bu has zero cross-section.

Summary

Thermal conductivity: the crossover from blue-down to electron domination occurs at $T/\mu_q \sim \alpha/7.7 \sim 10^{-3}$, so most of the temperature range of interest for neutron stars is in the blue-down-dominated regime where $\kappa \sim 1/T$.

Shear viscosity: the crossover from blue-down to electron domination occurs at $T/\mu_q \sim 10^{-5}$, so electrons are dominant down to $T \sim 10\,\mathrm{keV}$. The crossover temperature for the shear viscosity is much smaller than for the thermal conductivity because the relevant collisions for shear viscosity are those that transfer higher momentum, so the increase in the range of $\tilde{Q}$ interaction has a smaller impact on the mean free path since the long-range interactions involve low momentum transfer.

Electrical conductivity: this is a special case because the transported quantity is $\tilde{Q}$ charge, so the blue down quarks, which are $\tilde{Q}$ neutral, do not contribute to the electrical conductivity. The electron contribution therefore dominates over the entire temperature range.

Other possible excitations - the color-magnetic flux tubes and gluons in the unbroken gauge sector. Flux tubes are at sufficiently low temperature and high magnetic field, the vortex-fermion scattering via the Aharonov-Bohm effect may suppress the electron contributions to the electrical conductivity and shear viscosity.

IV. Cooling of NS and CCO in Cassiopea A

Chandra X-ray image of Cas A - the youngest (320 yr) SNR in the Milky Way.

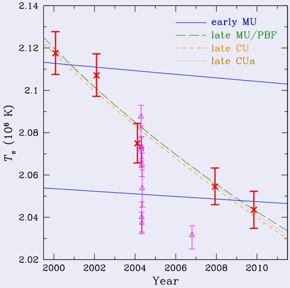

NASA's Chandra X-ray Observatory has discovered the first direct evidence for a superfluid. (Conclusions drawn from cooling simulations of the neutron stars).

Compact stars with dense quark cores: EoS, composition and evolution

A Sedrakian

Dense QCD and Compact Stars

Transport coefficients of dense quark matter: Variational calculation

Numerical and analytical results for 2SC phase

Summary

Cooling and Cas A data

Summary

Thermal history of C

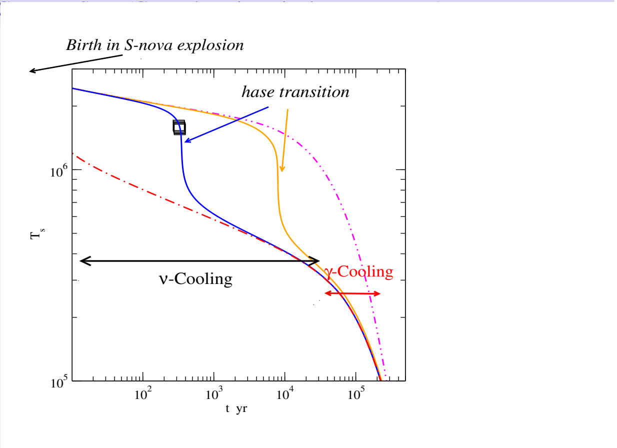

$$\boxed{\frac{\partial S}{\partial t} + \vec{\nabla}\cdot\vec{q} = \mathcal{R} - \mathcal{L}_\nu - \mathcal{L}_\gamma} \quad dS = c_V dT, \quad \vec{q} = \kappa\vec{\nabla}T$$

- Dissipative function $\mathcal{R} \propto \sigma(\nabla\phi)^2 + \kappa(\nabla T)^2/T + \ldots$
- Neutrino losses $\mathcal{L}_\nu$ from the bulk
- Photon losses $\mathcal{L}_\gamma$ from the surface

Phase transition within the QCD phase diagram can take place from one pairing pattern to the other (e.g. 2SC to Crystalline)

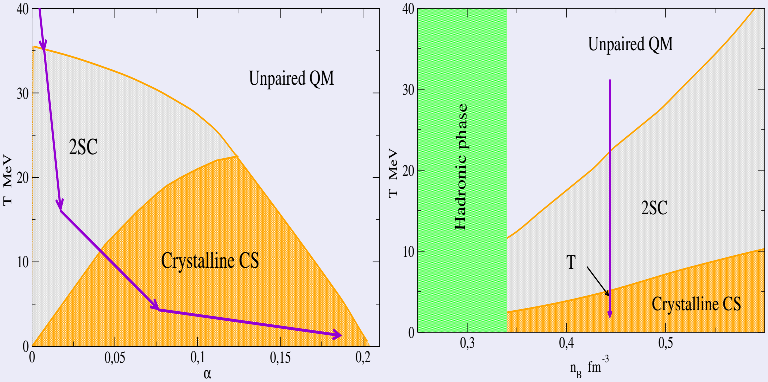

Left: Generic phase diagram of imbalanced fermi-systems; Right: β-equilibrated stellar matter

- 2SC phase - fully gapped, no excitations, ν-emission strongly suppressed
- gapless (or crystalline) phase ν-emission enhanced

In the red-green color sector

$$\zeta = \Delta_{rd}/\delta\mu, \qquad \delta\mu = (\mu_d - \mu_u)/2$$

and in the blue color sector

$$\Delta_b = 0 \qquad \Delta_b \neq 0.$$

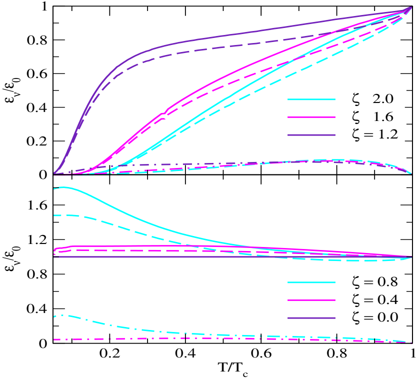

Figure : Upper panel: perfect 2SC phase $\zeta > 1$, Lower panel: crystalline phase $\zeta < 1$

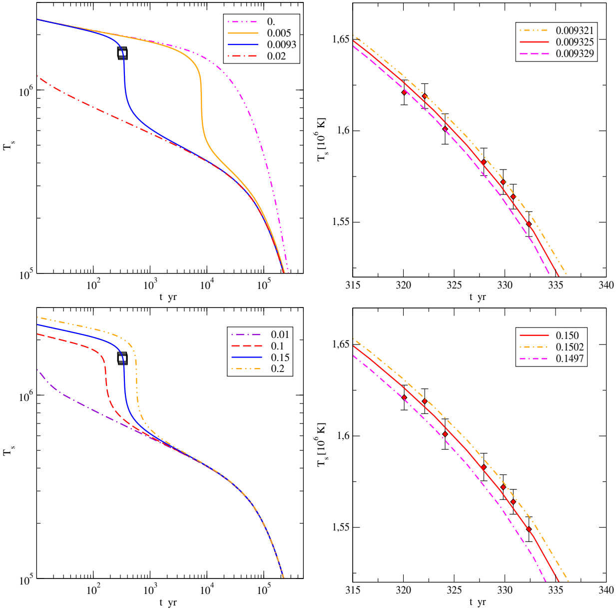

Fine tuned to the Cas A data using the phase transition temperature T^* and Δ_b.

Summary

- Better understanding of excitations and mechanisms of transport in 2SC phase
- Formalism which includes dynamical screening effects is general and can be applied to multi-component relativistic systems
- Cooling simulations indicate that Cas A behaviour can be understood as a phase transition in QCD phase diagram
- This comes, of course, with all the uncertainties of our current understanding of non-perturbative QCD - best phenomenology we can do in the year to come